Biophysical Chemistry 14 (1981) 159–176
Elsevier/North-Holland Biomedical Press

TWO-ENZYME ACTIVE TRANSPORT IN VITRO WITH pH INDUCED ASYMMETRICAL FUNCTIONAL STRUCTURES. III. DISCUSSIONS BASED ON NUMERICAL TREATMENTS OF THE TIME-DEPENDENT EVOLUTIONS

Jean-Claude VINCENT, Eric SELEGNY and Michel METAYER

Laboratory of Charged and reactive Polymers and of Biomimetics (E.R.A.471), Universite de Rouen, 76130 Mont-Saint-Aignan, France

Received 2 February 1981

Three complementary models have been considered in which pH gradients (step function, linear pH or linear H^+) impose asymmetry on a two-enzyme mixture. If the "combined pH dependences" of enzymes is pro-asymmetrical, the pH gradient induces an asymmetrical distribution of potential activities ("latent" asymmetry of functional structure). When substrate is added, "developed" asymmetry of effective activities appears which results in "substrate space wave" and pumping when the catalysed reaction couple is "inversible". It is shown that only one steady state exists for a given boundary condition and is attained when the "combined effective activity" of enzymes is nil: the stationary flux with symmetrical boundaries or the stationary load with moving boundaries is proportional to "effective global activities" of enzymes. "Equivalent square models" could be proposed that would be able to describe "functional" or "permanent" structure pumps as well. These models belong to the thermodynamic branch and the asymmetrical "space wave" substrate concentration profiles obtained must be distinguished from dissipative structures. It appears that such primary active transport pumps are chemical equivalents of heat pumps.

1. Introduction

In two papers, recently published in this journal [1,2], we gave the simplified analytical kinetic treatment and the experimental demonstration of a two-enzyme active transport pump induced by an asymmetrical pH gradient.

In this vectorial transport a "thick membrane" contained an isotropic mixture of enzymes of different pH dependences (γ_i). The direct effect of the pH gradient was the activation of a different enzyme in two different regions of the membrane (fig. 1a). This spatial distribution of "potential enzyme activities" [$V(E_i)$] was named the "asymmetrical functional structure". Such a structure depends on the relative pH dependences of the enzymes and is independent of the substrate.

It was also shown [1,3–6] that the energetic requirements and the necessary existence of a "sink reaction" (where the substrate S is consumed) and of a "source reaction" (where the substrate is produced) are met with "inversible" reaction couples: an irreversible reaction is coupled to a reversible one. In our case the transformation $S \rightarrow P$ is catalysed by enzyme E_1 and $P \rightarrow S$ by E_2.

When substrate is added to a system where the "asymmetrical functional structure" and an "inversible reaction couple" are united, "effective enzyme activities" (a function of substrate concentration) develop, and a "space-wave" type diffusion-reaction concentration profile and substrate pumping result.

The previous literature on in vitro active transport was already cited [1,3].

Here we want to show first that functional structures are quantified by the "potential enzyme activity profile" in the membrane. These profiles are calculated for various typical pH gradients in the "square model", the "linear pH profile model" and the "linear hydrogen-ion profile model". It must be mentioned that physical significance can be attached to each model as explained in fig. 1b

0301-4622/81/0000–0000/$02.50 © 1981 Elsevier/North-Holland Biomedical Press

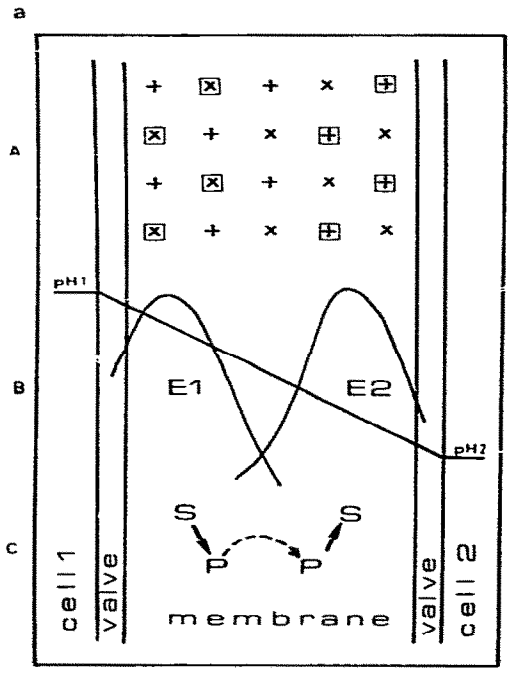

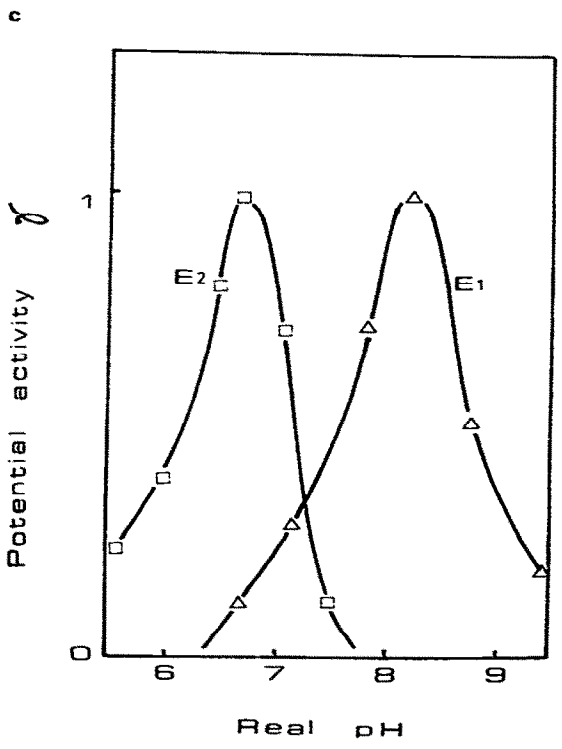

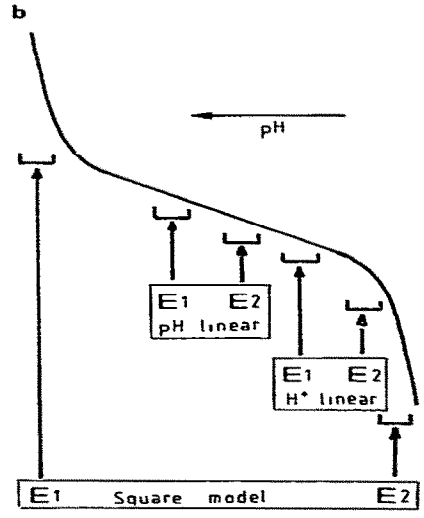

Fig. 1. (a) Schematic diagram of a two-enzyme active transport membrane in which the functional structure is induced by an external pH gradient: (A) homogeneously distributed enzymes E_1 and E_2; (B) pH dependence (γ_r) curves of both enzymes; (C) the inverse chemical reactions. (b) Physical significance of the three models. To a first approximation the pH profile in the membrane has the shape of the neutralization (dilution) curve of the diffusing, strong or weak acid or base used to regulate the enzyme membrane. If $\Delta pH = \Delta pH_{lim}$, according to the pH dependence (γ_r), curves one or other of the models becomes more adequate: (A) if enzyme E_1 is active when the pH is acid and E_2 when it is alkaline, the pH is virtually constant in each extreme layer of the membrane and we get the "square model"; (B) if E_1 and E_2 work at two different pH values but near pH=7 the pH is linear in the membrane and we get the "linear pH profile model"; (C) if the optimal pH values of both E_1 and E_2 are situated in the acid (or alkaline) region, the H^+ (or OH^-) concentration profile is linear in the membrane and we obtain the "linear H^+ concentration profile model". (c) Illustrative pH dependence (γ_r) curves of the two enzymes used in our experimental glucose pump [2]: hexokinase and acid phosphatase.

and legend. Further discussions on functional structures lead us to the important notion of "pro-asymmetry" linked to enzyme properties.

Secondly, space waves are calculated with different substrate concentration levels on the membrane boundaries. It will be shown that pumping properties are related to the "global" effective activity and not to the shape of its profile in the membrane.

With these results in hand, global or "equivalent" models may be proposed that are able to distinguish evolutions and steady states but regroup the "functional" and "permanent" [3] structures that are able to pump.

To make the calculations and discussions possible, new notations including the potential and effective enzyme activities are used. The present treatment is not limited to steady states or to reactions of even order; complexity arises from less restrictive assumptions and requires numerical treatments. Such treatment of mono- or poly-enzymatic immobilized enzyme systems using dimensionless parameters was initiated in 1971 in our laboratory [7]. The method has been widely developed and mathematically justified [8] and is now currently used.

Past experience in the field has shown how essential it is to verify the singleness of the steady state that appears at the end of the spontaneous establishment period, by solving the nonlinear differential equations of time evolutions numerically. In this respect no guarantee is offered by linearized solutions.

2. Notations and models

2.1. Notations

(See symbols in table 1.) In agreement with refs. [5,6,9,10] the local reaction rate $(v_i)_{x,t}$ at time t and space coordinate x along an axis perpendicular to the plane of the membrane ($0 \leqslant x \leqslant 1$) is written:

$$(v_i)_{x,t} = V_{mi}(\gamma_i \lambda_i)_{x,t}, \tag{1}$$

where V_{mi} is the maximum velocity; γ_i is the mathematical expression of the pH dependence of enzyme E_i, its value varies between 0 and 1 and is maximum for the optimal pH; the function λ_i expresses the substrate dependence, for Michaelian enzymes it takes the form

$$\lambda_i = S_i/(K_{mi} + S_i) = s_i/(1 + s_i)$$

(K_{mi} = Michaelis' constant. S_i = substrate concentration and $s_i = S_i/K_{mi}$). λ_i varies also from 0 to 1 while the substrate concentration increases from 0 to the saturating value.

If σ_i is the characteristic "Thiele type" dimensionless enzyme diffusion-reaction parameter of the membrane ($\sigma_i = V_{mi}e^2/K_{mi}D$; D = diffusion coefficient of S; e = thickness of membrane), the "local potential activity" is defined by

$$v(E_i)_{x,t} = (\sigma_i \gamma_i)_{x,t} \tag{2}$$

and the "local effective activity" is

$$v(\mathfrak{S}_i)_{x,t} = (\sigma_i \gamma_i \lambda_i)_{x,t}. \tag{3}$$

It can be seen that for $\lambda_i = 1$ (high substrate concentrations), $v(\mathfrak{S}_i)_{x,t} = v(E_i)_{x,t}$, in other words the potential enzyme activity represents the maximum enzyme activity under the local pH conditions and is particularly useful for following the effect of pH, disregarding that of the substrate.

For isotropic membranes σ_i is constant in space and time; and, by integration throughout the whole membrane, we obtain for each enzyme the expression of the "global potential activity":

$$V(E_i)_t = \sigma_i \int_0^1 (\gamma_i)_{x,t}\, dx \tag{4}$$

and of the "global effective activity"

$$V(\mathfrak{S}_i)_t = \sigma_i \int_0^1 (\gamma_i \lambda_i)_{x,t}\, dx. \tag{5}$$

In the following, we do not consider pH modifications due to reaction products (neutral reactions or strong buffering) and for each model the pH through the membrane is assumed to be independent of time, consequently each $(\gamma_i)_{x,t}$ reduces to $(\gamma_i)_x$. With these assumptions the potential activity profiles and the global potential activities are constant ($V(E_i)_t = V(E_i) = Ct^e$).

In the inversible enzyme reaction the activities of the couples E_1 and E_2 have inverse effects on the S or P concentration and the local tendency to

Table 1
List of symbols

a	Membrane surface area
b_i, c_i	Coefficients of the $\gamma_{1,2}$ eqs. (9), (21)–(24)
D	Diffusion coefficient of S and P in the membrane
e	Membrane thickness
J_s	Diffusion-reaction flux of S
K_m	Michaelis constant of E_1 and E_2 enzymes
m	Optimal value of rationalized ΔpH: $m=\Delta pH/\Delta pH_{lim}$
n	Relative inactive layer thickness in the square model
pH	Cologarithm of the H^+ concentration
pH_a	Intermediate pH value for which $\gamma_{1,2}=0$
P, p	Real and adimensional product concentration: $p=P/K_m$
S, s	Real and adimensional substrate concentration: $s=S/K_m$
t, t'	Real and adimensional time: $t'=tD/e^2$
v_i	Enzymic reaction rate of E_i: $v_i=V_{mi}\gamma_i\lambda_i$
$v(E_i)$	Local potential enzyme activity: $v(E_i)=\sigma_i\gamma_i$
$v(\mathcal{E}_i)$	Local effective enzyme activity: $v(\mathcal{E}_i)=\sigma_i\gamma_i\lambda_i$
v_m	Membrane volume: $v_m=ae$
v_{cj}	Volume of the cell compartment: $j=1$ or 2
V_{mi}	Maximum rate of reaction catalyzed by E_i (at optimal pH)
$V(E_i)$	Global potential enzyme activity: $V(E_i)=\int_0^1 v(E_i)\,dx$
$V(\mathcal{E}_i)$	Global effective enzyme activity: $V(\mathcal{E}_i)=\int_0^1 v(\mathcal{E}_i)\,dx$
X, x	Real and adimensional distance parameter: $x=X/e$
Z	Concentration of the species Z
λ_i	Substrate dependence of enzyme E_i
γ_i	pH dependence of enzyme E_i
$\gamma_{1,2}$	Combined pH dependence of enzyme couple E_1 and E_2
Δx	Space increment
Δt	Time increment
ΔpH	pH interval between $x=0$ and $x=1$
ΔpH_{lim}	Active zone: between both extreme roots of eq. (9)
σ_i	Dimensionless diffusion-reaction parameter of the membrane: $\sigma_i=V_{mi}e^2/K_mD$, related to enzyme E_i, $i=1$ or 2.

consume S or produce P is given by the "combined potential activity":

$$v(E_{1,2})_x = v(E_1)_x - v(E_2)_x = (\sigma_1\gamma_1 - \sigma_2\gamma_2)_x$$
$$= \sigma_1(\gamma_1 - \alpha\gamma_2)_x = \sigma_1(\gamma_{1,2})_x, \qquad (6)$$

where $\gamma_{1,2}=\gamma_1-\alpha\gamma_2$ and $\alpha=\sigma_2/\sigma_1$. An evident simplification consists of assuming $\sigma_1=\sigma_2=\sigma$ leading to

$$\gamma_{1,2} = (\gamma_1 - \gamma_2)_x. \qquad (7)$$

If $\gamma_{1,2}>0$ S is consumed and if $\gamma_{1,2}<0$ S is produced when the initial P concentration is not much higher than that of S. As active transport of the types studied needs the association of a reactive "sink" and of a "source", $(\gamma_{1,2})_x$ *must change its sign* inside the membrane. This condition expresses the necessary interrelation between the γ_1 and γ_2 functions of the enzymes and the ΔpH to be imposed on the membrane boundaries, in order to obtain the "functional structure" needed. (In other words the space asymmetry of enzyme activities under a pH gradient is already memorized in the intrinsic *pro-asymmetry* of the γ_i of the selected enzymes.)

The combination with the local S and P concentrations gives the "local combined effective activity"

$$v(\mathcal{E}_{1,2})_{x,t} = v(\mathcal{E}_1)_{x,t} - v(\mathcal{E}_2)_{x,t}$$
$$= \sigma(\gamma_1\lambda_1 - \gamma_2\lambda_2)_{x,t}. \qquad (8)$$

Integration of eq. (8) throughout the membrane gives the "global combined effective activity" $V(\mathcal{E}_{1,2})_r$.

In addition to the above quantities the following dimensionless ones are also used: space, $x = X/e$; time, $t' = tD/e^2$; we assume similar D values for the diffusion coefficients of S and P.

2.2. Models

Each model examined is characterized by the mathematical expression of its $\gamma_{1,2}$ profile as a function of x, $\gamma_{1,2}(x)$.

In the "square model", $\gamma_{1,2}(x)$ is a step function; the membrane is divided into three layers [1,2]: (i) two layers of identical thickness $e/(n+2)$ and inverse activities corresponding to $\gamma_{1,2}(x) = +1$ for $x < 1/(n+2)$ and $\gamma_{1,2}(x) = -1$ for $x > (n+1)/(n+2)$; (ii) an intermediate inactive layer of thickness $ne/(n+2)$ where $\gamma_{1,2}(x) = 0$ for $1/(n+2) < x < (n+1)/(n+2)$. n is a variable of the

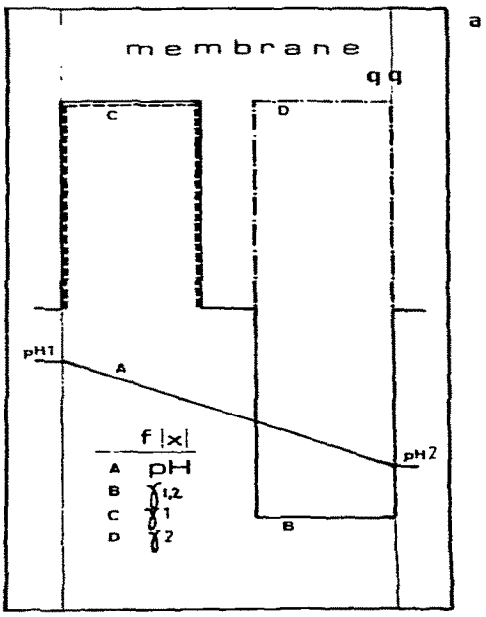

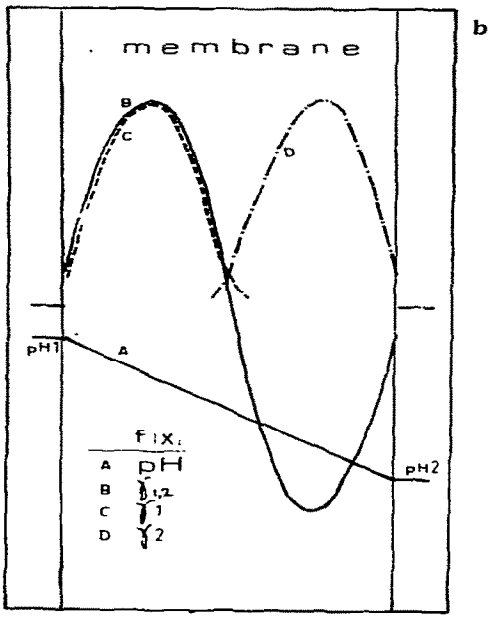

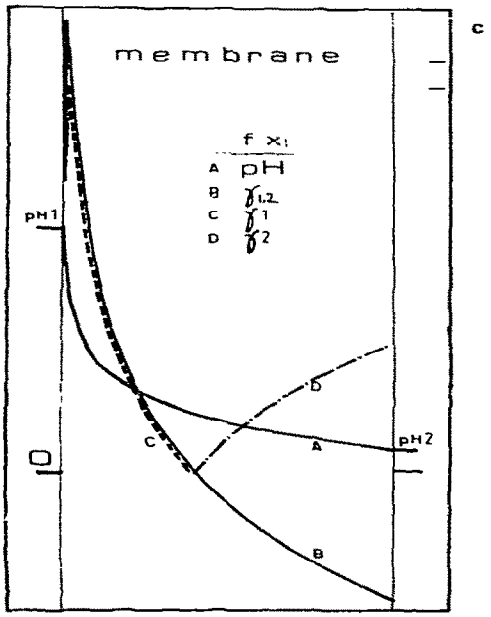

Fig. 2. The three models with: (A) pH profile inside the membrane pH(x); (B) the combined potential activity profile $\gamma_{1,2}(x)$; (C) the potential activity profile $\gamma_1(x)$ of E_1; (D) the potential activity profile $\gamma_2(x)$ of E_2. (a) The square model; (b) the linear pH profile model; (c) the linear H^+ concentration profile model.

external pH values at the membrane limits (fig. 2a). This is a limiting mean approximation of the potential enzyme activity profiles generated by a pH gradient in the membrane.

The effect of the pH gradient can be more accurately expressed by combining the pH profile at a given moment $\mathrm{pH}(x)$ with the combined potential activity $\gamma_{1,2}$ (pH), thus obtaining the potential enzyme activity profile

$$\gamma_{1,2}(\mathrm{pH}(x)).$$

In agreement with eq. (7) if the pH-dependence laws γ_i of the participating enzymes are parabolic or gaussian and overlap each other [9,10] (fig. 1c), a satisfactory approximation of $\gamma_{1,2}(\mathrm{pH}(x))$ is given by a polynomial expression of third degree:

$$\gamma_{1,2}(\mathrm{pH}(x)) = b_0 + b_1\,\mathrm{pH}(x) + b_2\,\mathrm{pH}^2(x) + b_3\,\mathrm{pH}^3(x). \quad (9)$$

$\gamma_{1,2}((\mathrm{pH})) = 0$ for the three roots of eq. (9); physical significance exists only for pH values situated between the smallest and the greatest root: the pH interval between these values is $\Delta\mathrm{pH}_{\mathrm{lim}}$ and enzyme activity only exists in this pH zone. The pH values on membrane boundaries ($x = 0$, $x = 1$) will always be included between these values or, in other terms, inactive layers near the boundaries are not considered.

The intermediate root corresponds to pH_n for which the combined potential activity is nil (equal potential activities).

From the experimental $\gamma_{1,2}$ ((pH)) of the enzyme couple the b_i coefficients are easily obtained by numerical fitting; the hexokinase-acid phosphatase couple is given as an example in fig. 1c. (If the γ_i of the studied enzyme couple were more widely separated, a 5th degree relation could be used.)

In the "linear pH profile model" the variation of the pH is assumed to be proportional to space coordinate x:

$$\mathrm{pH}(x) = \mathrm{pH}(0) + x\big[\mathrm{pH}(1) - \mathrm{pH}(0)\big]. \quad (10)$$

The illustration given in fig. 2b shows that we need to fix $\mathrm{pH} = \mathrm{pH}_n$ at $x = 0.5$ in order to get $V(\mathrm{E}_1) = V(\mathrm{E}_2)$. The midpoint is a symmetry point of $\gamma_{1,2}(x)$.

In the "linear H^+ ion concentration profile model" the H^+ concentration is a direct function of x,

$$\mathrm{pH}(x) = -\log\big\{H(0) + x\big[H(1) - H(0)\big]\big\}. \quad (11)$$

The example of fig. 2c shows that $V(\mathrm{E}_1) = V(\mathrm{E}_2)$ is obtained with an asymmetrical $\gamma_{1,2}(x)$ profile, as a consequence of the logarithmic relation between the pH and the H^+ concentration.

3. The mathematical treatment

3.1. The equations to be solved

Applying the general equation of diffusion reactions for a species Z (Z = S or Z = P):

$$(\mathrm{d}Z/\mathrm{d}t)_{x,t} = (\partial Z/\partial t)_{x,t}\ \text{diffusion} + (\partial Z/\partial t)_{x,t}\ \text{reaction} \quad (12)$$

and introducing Fick's law and Michaelian kinetics [1] we have the now classical relations, for the substrate:

$$\partial s/\partial t' = \partial^2 s/\partial x^2 - v(\mathfrak{S}_{1,2})_{x,t'} \quad (13)$$

and for the product:

$$\partial p/\partial t' = \partial^2 p/\partial x^2 + v(\mathfrak{S}_{1,2})_{x,t'}. \quad (14)$$

3.2. The numerical treatment

In the numerical analysis the partial differentials of $s_{x,t'}$ are assimilated to small modifications of the function due to elementary variations of the space and time variables using two major techniques: the implicit method and the explicit method [7,8]. In the first case the partial differentials relative to space are calculated at time $t' + \Delta t'$ (unknown profile) and in the second case at time t' (known profile). The corresponding equations are, for example, for substrate:
With the implicit method:

$$s_{x+\Delta x}^{t'+\Delta t'} = 2s_x^{t'+\Delta t'} - s_{x-\Delta x}^{t'+\Delta t'} + \Delta x^2\Big[\big(s_x^{t'+\Delta t'} - s_x^{t'}\big)/\Delta t' + v(\mathfrak{S}_{1,2})_x^{t'+\Delta t'}\Big]. \quad (15)$$

With the explicit method:

$$s_x^{t'+\Delta t'} = s_x^{t'} + \Delta t' \left[\left(s_{x+\Delta x}^{t'} + s_{x-\Delta x}^{t'} - 2s_x^{t'} \right) / \Delta x^2 - v(\mathfrak{S}_{1,2})_x^{t'} \right], \quad (16)$$

for the product we get

$$p_x^{t'+\Delta t'} = p_x^{t'} + \Delta t' \left[\left(p_{x+\Delta x}^{t'} + p_{x-\Delta x}^{t'} - 2p_x^{t'} \right) / \Delta x^2 + v(\mathfrak{S}_{1,2})_x^{t'} \right], \quad (17)$$

with the condition of stability and singleness:

$$\Delta t'/\Delta x^2 < (2 + \sigma \Delta x^2)^{-1}. \quad (18)$$

Because of the number of steps imposed by the $\Delta t'$ condition of eq. (18) the explicit method requires more computer time, but it is easier to handle, more especially when the orders of magnitude of the concentration of the species considered are different. Most of the results presented here were obtained by this technique with a powerful computer system.

Step-by-step computations of the concentration profiles of the different species in the membrane were obtained for preselected Δx and $\Delta t'$ values, i.e., as a function of space and time and from there the fluxes were calculated. In the absence of analytical expressions the results are expressed in graphic form as usual.

3.3. Computing

Two different computing techniques were used: (i) a small Hewlett Packard model 15 (HP 9815) computer with a capacity of 2000 programme steps coupled to a magnetic tape memory and to an *X-Y* tracer; (ii) a large system including two IBM 370-168 computers with a capacity of 7 million octets belonging to the computer center of CIRCE in Orsay and connected by a terminal to our university.

4. Results

The results for the three models are given successively; however, several properties, except for the pH-activity relations, are shared by all of them. In order to avoid unnecessary repetition of trivial equivalences we shall examine complementary properties in the different models and look for more general views in the conclusion.

4.1. The square model: $\gamma_{1,2}$ (x) is a step function

With this simplified model we already had some analytical results [1] limited to steady-state conditions. We are interested in the rate of evolution of substrate concentrations and fluxes without forgetting that at infinite time the analytical and numerical analyses must come to the same result, except for the intermediate order reaction rates.

4.1.1. The steady state with fixed boundary conditions: its establishment and singleness

As indicated by the analytical treatment [1], the steady state with fixed membrane boundaries is the same as the first quasi-stationary state obtained with moving boundaries (before any change in cell concentration occurs).

This is also the first state after the initial one at $t = 0$ that can be identified by exact analysis and we expect numerical treatments to give us some more information on the establishment period before the steady state. Starting with a void or a full membrane we find at zero order the following results:

Originally void membrane. The membrane is assumed to be activated by the pH gradient before the substrate is added in the compartments. It is shown in fig. 3a that the substrate space wave is progressively generated before any further change.

Originally full membrane. It is assumed that the membrane is filled by substrate before being quickly activated by the pH gradient. In this case the space wave is rapidly generated and is simultaneously amplified on both sides of a central symmetry point (fig. 3b), as contact time increases.

The most important conclusion is that the steady-state profile is the same in both cases; there is singleness of this state, under identical boundary conditions *independently of filling and activation sequences.*

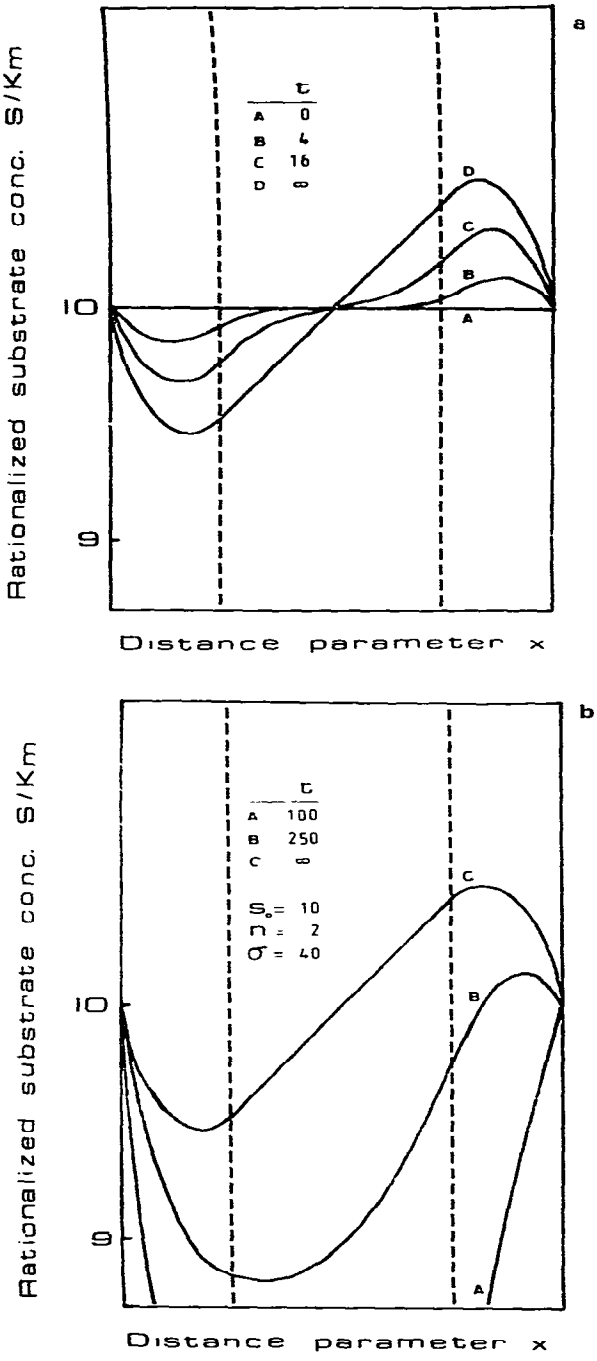

Fig. 3. Square model: singleness of the steady state with imposed boundaries; (a) membrane initially void of substrate; (b) membrane initially full of substrate.

4.1.2. Establishment and existence of a unique first quasi-stationary state with moving boundaries

With finite cell volumes (v_{cj}) ($j = 1$ or 2) on both sides of the membrane the transport of substrate modifies the concentration in the compartments. The substrate diffusion flux at each point of the membrane is

$$J_s = -D \operatorname{grad} S. \tag{19}$$

This flux through membrane surface "a" is proportional to the tangent of the concentration profile at $s(0)$ on the input side (where $x = 0$) and at $s(1)$ on the output face (where $x = 1$). The elementary rate of modification of the concentration in compartment j follows the law

$$\Delta s_j = (v_m / v_{cj})(\Delta s / \Delta x)_{x=j} \Delta t', \tag{20}$$

where $v_m = ae$ is the membrane volume.

The calculations illustrated in fig. 4a show the evolution of the system toward the steady state where the entering and leaving fluxes become nil.

These results have further implications; they demonstrate that in order to work the membrane must first be filled with substrate in a manner identical to the steady state obtained with fixed boundaries. After that, due to quick relaxation inside the membrane, the evolution goes through successive quasi-stationary states caused by the modifications of boundary concentrations controlled by the pumping itself (fig. 5).

It can be again concluded that the pumping starts with a *unique and real quasi-stationary state* which is the same as that given by the analytical approach; this previously assumed state is now justified.

The influence of the initial product concentration was also obtained. Once the pumping is established the S and P concentrations are of the same order of magnitude* (figs. 5 and 11a) and

* This means that if $k_{m1} \neq k_{m2}$ the orders of the two reactions are similar in the steady state as was assumed in the analytical model [1].

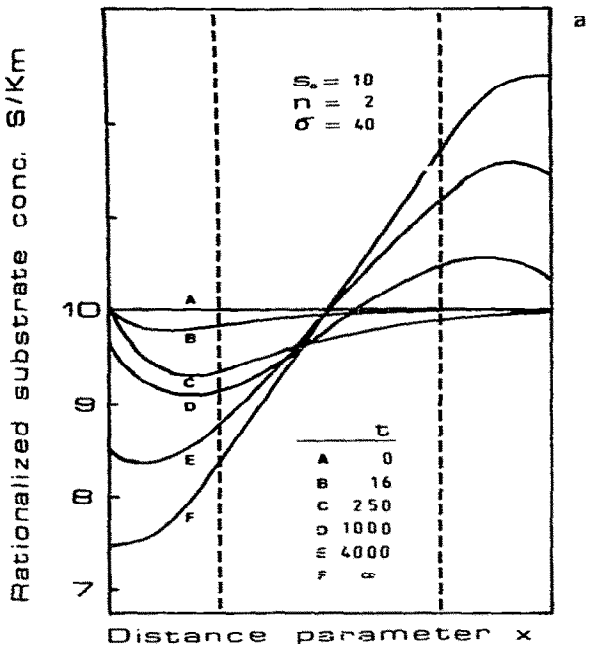

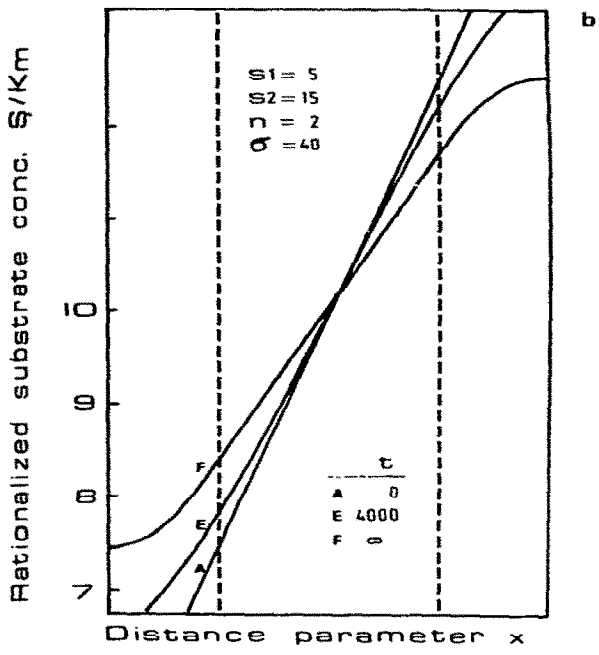

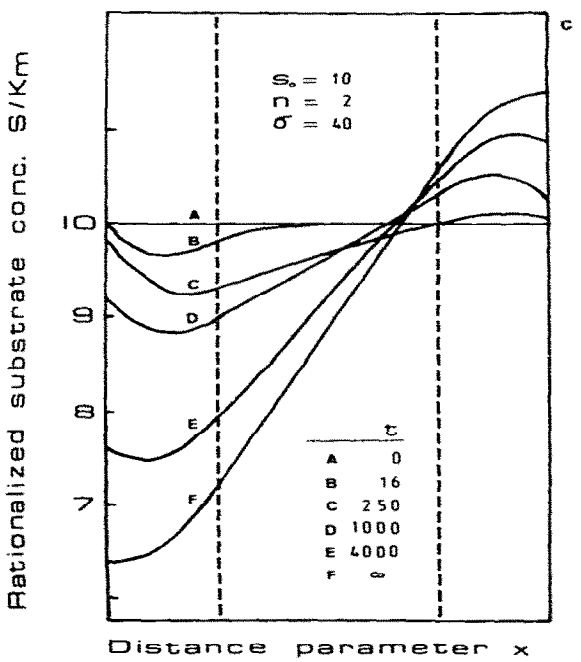

Fig. 4. Square model: singleness of the steady state with moving boundaries: (a) membrane initially full of substrate and void of product; (b) active barrier with initial substrate concentration gradient higher than the maximum load of the pump; (c) unequal cell volumes with $v_{c2}/v_{c1} = 3$.

the resulting steady state is largely independent of the initial P concentration.

4.1.3. The membrane as an "active barrier"

If we now consider an initial boundary concentration difference which is higher than the maximum load of the pump, the passive back-diffusion flux of substrate will exceed the active flux and (with moving boundaries) the gradient tends toward its steady state following apparently passive diffusion kinetics.

The stationary state load Δs_{max} (fig. 4b) is the same as with an "uphill pumping" approach.

The stationary state is also independent of the initial conditions at the membrane boundaries.

4.1.4. The size of the compartments

The compartment volumes change the rate of

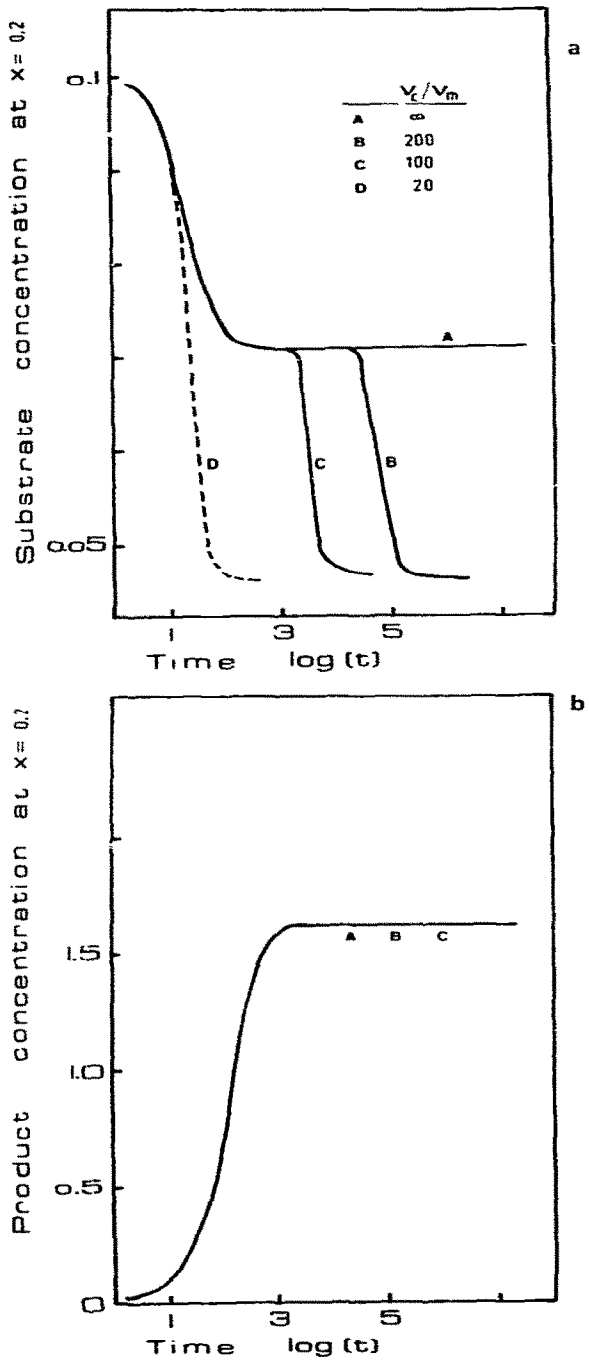

obtaining the steady state to a great extent, but do not change the corresponding maximum load (fig. 4c). However, if the reservoir on the donor side is small, the pumping activity decreases the donor substrate concentration and the order of reaction starting at zero may increase up to one. The final gradient and the evolution toward the steady state undergo corresponding modifications.

4.2. The linear pH-profile model (fig. 2b)

The functional structure of potential activities is characterized by eqs. (9) and (10). Most of the conclusions obtained with the "square model" concern the establishment of the steady states and the effects of σ and of initial conditions. They do not undergo very significant changes with a linear pH activation. Two questions need further examination: the ΔpH-activity relation and the "equivalent model".

4.2.1. The control of global potential activities by the pH gradient

Let the pH gradient be centered at the $x = 0.5$ midpoint on pH_n (no net potential activity), a $V(E_1) = V(E_2)$ distribution of potential enzyme activities is obtained for all pH gradients (see figs. 2b and 1c).

As $V(E_i)$ represents the global potential activity as well as the corresponding maximum effective activity for membranes saturated with the substrate ($\lambda = 1$), the $V(E_i) = f(\Delta pH)$ relation gives simultaneous information on the variations of potential activity and on the zero-order pumping efficiency according to the pH gradient. As shown in fig. 6, with a flat symmetrical pH profile there is no enzyme and pumping activity. The enzyme activities and the pumping efficiency increase in proportion to the pH gradient up to a limit, after

Fig. 5. Square model: establishment and existence of a quasi-stationary state in a membrane with moving boundaries and different v_m/v_c values: evolution as a function of time in the plane $x = 0.2$ of: (a) substrate concentration; (b) product concentration. Curve D (a) gives an example of the non-existence of the quasi-stationary state when v_m/v_c is not sufficiently small. $s_0 = 0.1$; $p_0 = 0$; $\sigma = 20$.

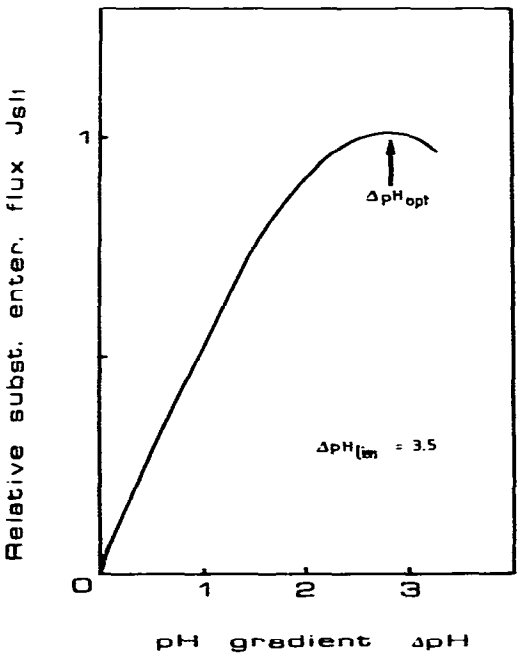

Fig. 6. Linear pH profile model: pumping activity as a function of the activating pH gradient; the total active zone is $\Delta pH_{lim} = 3.5$.

which both decline giving evidence of an optimal ΔpH value for $\Delta pH \simeq 0.8\Delta pH_{lim}$. This result can be demonstrated.

Expression of $\gamma_{1,2}(x)$ as a function of $pH - pH_n$ based on eqs. (9) and (10) results in a polynomial of odd third degree:

$$\gamma_{1,2}(x) = c_1x^3 + c_2x \tag{21}$$

its roots are 0, A and $-A$, c_1 and c_2 are constants and the total activity Q is proportional to the surface covered by this curve when $\Delta pH = \Delta pH_{lim}$ in the membrane:

$$Q = c_1x^4/4 + c_2x^2/2 \tag{22}$$

for a smaller ΔpH we have $x = mA$; for the whole thickness of the membrane the corresponding activity is:

$$V(E_{1,2}) = c_1m^3A^4/4 + c_2mA^2/2 \tag{23}$$

$V(E_{1,2})$ is maximum when:

$$m^2 = -2c_2/3c_1A^2 \tag{24}$$

A being a root of eq. (21) we have $A^2 = -c_2/c_1$ and after substitution in relation (24):

$$m = \sqrt{2/3} \simeq 0.81 \tag{25}$$

This result is in reasonable agreement with that of fig. 6 and we understand that the pumping activity is a function of the σ value taken by the membrane independent of the shape of the pH gradient that produces it.

4.2.2. The "equivalent square model"

Using the last remarks of the preceding section, an equivalent square model with its σ and with general properties similar to those of the original linear pH model can be calculated. For two enzymes whose pH activities overlap we have $n = 0$ and σ is obtained from eq. (23):

$$\sigma = c_1m^3A^4/4 + c_2mA^2/2$$

where $A = \Delta pH_{lim}/2$, $m = \Delta pH_{lim}$ and c_1 and c_2 are furnished by experiments or numerical fitting.

In agreement with the assumptions used to construct this model the $\gamma_1(x)$ and $\gamma_2(x)$ are symmetrically distributed and the equivalent square model is also symmetrical.

4.3. The linear H^+ concentration profile model (fig. 2c)

Consider an uncharged membrane and asymmetry imposed by diffusion of an acid (or a base) between fixed boundaries; the steady-state H^+ (or OH^-) concentration profile through the membrane will be linear, the pH profile logarithmic and the corresponding $pH(x)$ and enzyme activity profiles very asymmetrical; eqs. (9) and (11) and fig. 2c describe this situation.

The modification of the acid gradient changes the $pH(x)$ and consequently the $V(E_{1,2}(x))$ functions but the principles of the mathematical treatment remain the same as before. From now on, we shall concentrate on steady-state fluxes.

4.3.1. Substrate flux-substrate concentration relationship is not Michaelian

With a constant σ the shape of the curve representing the steady-state active transport flux for various identical external dimensionless concentrations s_0 at first sight seems similar to that of the Michaelian kinetics. Effectively, this flux is proportional to s_0 for small concentrations ($s_0 < 0.3$) and levels off for high ones ($s_0 > 10$). However, a more rigorous examination of the substrate flux-substrate concentration relationship (fig. 7) shows that the saturation is retarded compared to Michaelian predictions; thus the combination of two Michaelian phenomena is not rigorously Michaelian. This observation is of interest to physiologists studying in vivo transport *.

The saturation level is not a function of V_m/K_m as in enzyme solutions but of σ which is also dependent on the diffusional characteristics of the membrane (e^2/D). Some analogy with the Michaelian law exists as the pumping activity is a linear function of small σ values and reaches a maximum when σ is high (fig. 8). However, the upper limit corresponds to full diffusion control of the intramembrane phenomenon and appears when the transformation of the substrate entering the membrane is nearly instantaneous and its concentration in the layer with E_1 activity approaches zero. (Reasonably, such a system should not be considered without the unstirred layer "film control" on the boundaries that would unavoidably appear even with efficient stirring in the compartments [11].)

4.3.2. The s(x) profile without a uniform order of reaction in the membrane

Let us consider first symmetrical fixed boundaries and a diffusion-reaction activity σ high enough to depress deeply the substrate concentration profile for low x values (near the entering face of the membrane). Along this profile the order of reaction increases with x, for example, from zero at the surface (if $s_0 > 10$) toward one inside the membrane, but at high x, E_2 and not E_1 is active.

* Examination of this question was promoted by Professor M. Thellier.

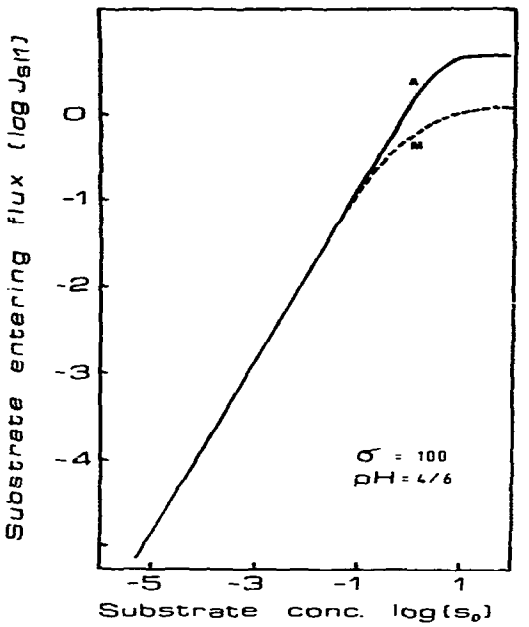

Fig. 7. Linear H^+ concentration model with fixed boundaries: entering substrate flux (logarithmic scale) due to pumping activity as a function of the external substrate concentration.

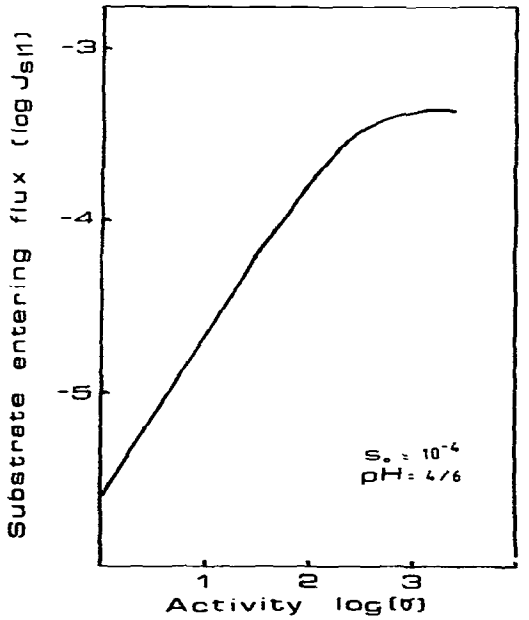

Fig. 8. Entering substrate flux (same as in fig. 7) as a function of the potential enzyme activities.

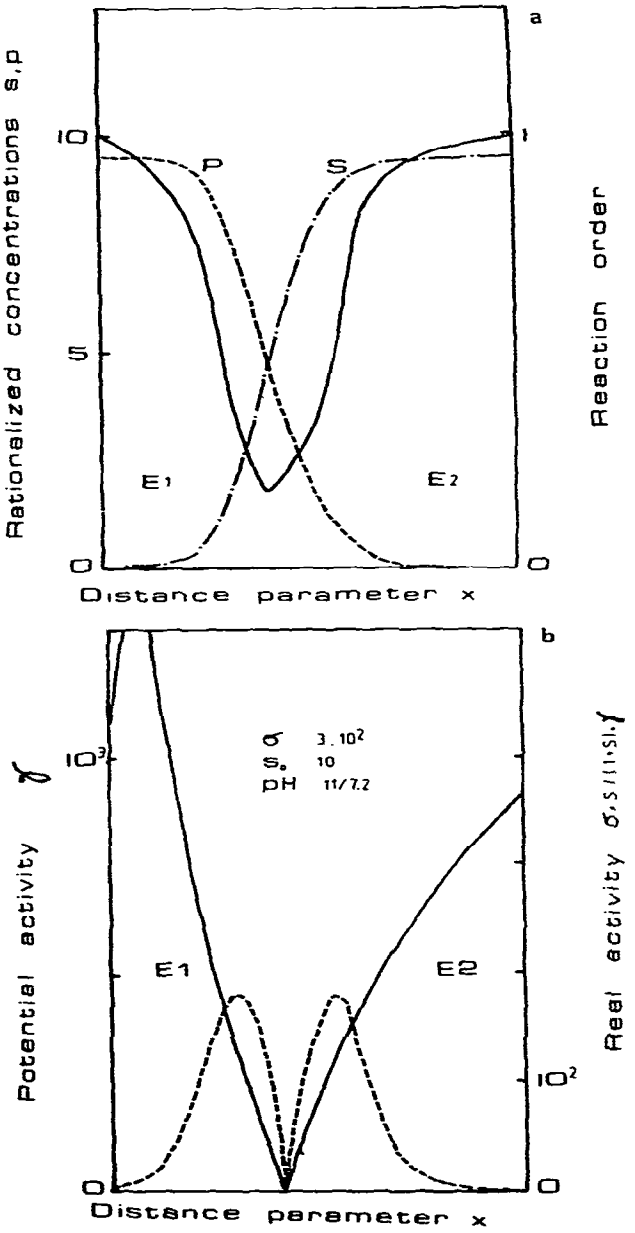

Fig. 9. Non-uniform order of reaction inside the membrane: (a) S and P concentration profile (left ordinate) and order of reaction (right ordinate); (b) potential (————) and effective (— — —) enzyme activity profiles; optimal pH values are 11 (E_1) and 7.2 (E_2); $\sigma = 3.10^3$.

and $s(x)$ and the order of reaction both increase again. The space wave is somewhat modified compared to purely zero- or purely first-order reactions, that is the zero-order profile is attenuated.

In the zero-flux steady state the boundary substrate concentrations are dissymmetrical and $s(x)$ and $p(x)$ profiles complementary to each other are found. If σ has a high value the concentration gradients are very abrupt, λ_1 and λ_2 are markedly dependent on x and their sum exhibits a low minimum as shown in fig. 9a. The $\lambda_1(x)$ and $\lambda_2(x)$ regulate the $V(\mathcal{E}_i(x))$ and the order of reaction profiles.

4.3.3. Potential and effective activities: combined effects of H^+ and S profiles

A variety of pH couples can be imposed on the membrane limits between which a linear H^+ profile induces equal global potential enzyme activities $V(E_1) = V(E_2)$. For a given enzyme couple the effective activity profiles $V(\mathcal{E}_i)_{x,t}$ are dependent on substrate (and product) concentration profiles and are different from potential activity profiles if the activity is not saturated.

An illustration of such profiles is given in fig. 9b for asymmetrical steady-state boundary conditions detailed in section 4.3.2. It is observed that the effective activity profile is asymmetrical but the surface covered by the curves, i.e., the effective activities $V(\mathcal{E}_1)$ and $V(\mathcal{E}_2)$ remain equal.

To explore this result further, calculations have been made for very different situations, some of which are given in table 2 where low but symmetrical boundary substrate concentrations were used.

Here again whatever the limiting pH values, the shape of potential activity profiles and even the proportions of potential activities, the global effective activities of the two enzymes are found to be equal in the steady state. This very fundamental observation reveals that this type of pump is self-regulating, self-stabilizing, and its evolutions toward the steady state are expressed by the evolution toward global $V(\mathcal{E}_{1,2}) = 0$.

4.3.4. Flux-effective activity relation

Table 2A and B shows that the substrate flux is directly proportional to the global effective activity and is independent of the means used to obtain

Table 2

Steady-state active transport fluxes of a membrane; enzymes: E_1 with $pH_{opt} = 8$, active pH zone: 8 ± 1; E_2 with $pH_{opt} = 10$, active pH zone: 10 ± 1. The potential activity is dependent on the difference between pH_1 and pH_2 values on membrane limits. Infinite cell volumes (fixed boundaries); external substrate concentration: $S_0 = 10^{-4} K_m$ in both cells.

	pH_1/pH_2	Shape of potential activity profile	Global potential activities		Global effective activities		Stationary flux (arbitrary units)
			$V(E_1)+V(E_2)$	$\%V(E1)$	$V(S_1)+V(S_2)$	$\%V(S_1)$	
A	7.00/9.40		32.66	50	0.0023	50	0.113
	7.50/9.39		31.76	50	0.0022	50	0.111
	8.00/9.36		29.08	50	0.0021	50	0.105
	8.50/9.28		21.09	50	0.0016	50	0.084
B	7.00/9.40		32.66	50	0.0023	50	0.113
	7.50/9.39		32.66	50	0.0023	50	0.113
	8.00/9.36		32.66	50	0.0023	50	0.113
	8.50/9.28		32.66	50	0.0023	50	0.113
C	7.00/9.40		32.66	50	0.0023	50	0.113
	7.00/9.25		32.66	78	0.0025	50	0.148
	7.00/9.55		32.66	27	0.0016	50	0.083

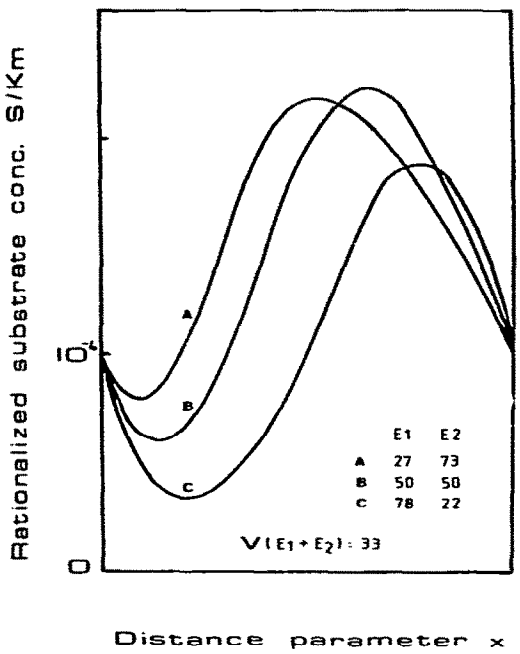

Fig. 10. Linear H^+ concentration profile model with imposed boundaries. Influence of the pH gradient; substrate concentration profiles with different global potential activity balances of the two enzymes E_1 and E_2.

these activities, namely with less enzyme and a strongly activating H^+ gradient or more enzyme and less favorable activation.

In table 2c the sum of all global potential activities is constant but their ratio is variable. It is seen that, within the limits explored, $0.25 < V(E_1)/(V(E_1)+V(E_2)) < 0.78$, the effective activity and the flux increase when $V(E_1)$ increases. A low $V(E_1)$ with a higher $V(E_2)$ is not at all favorable to pumping. This effect is explained by the large increase in product concentration inside the membrane (fig. 10), so that E_2 may work with a lower order of reaction and a higher efficiency than E_1.

4.3.5. The equivalent asymmetrical square model

In the steady or quasi-stationary states, the

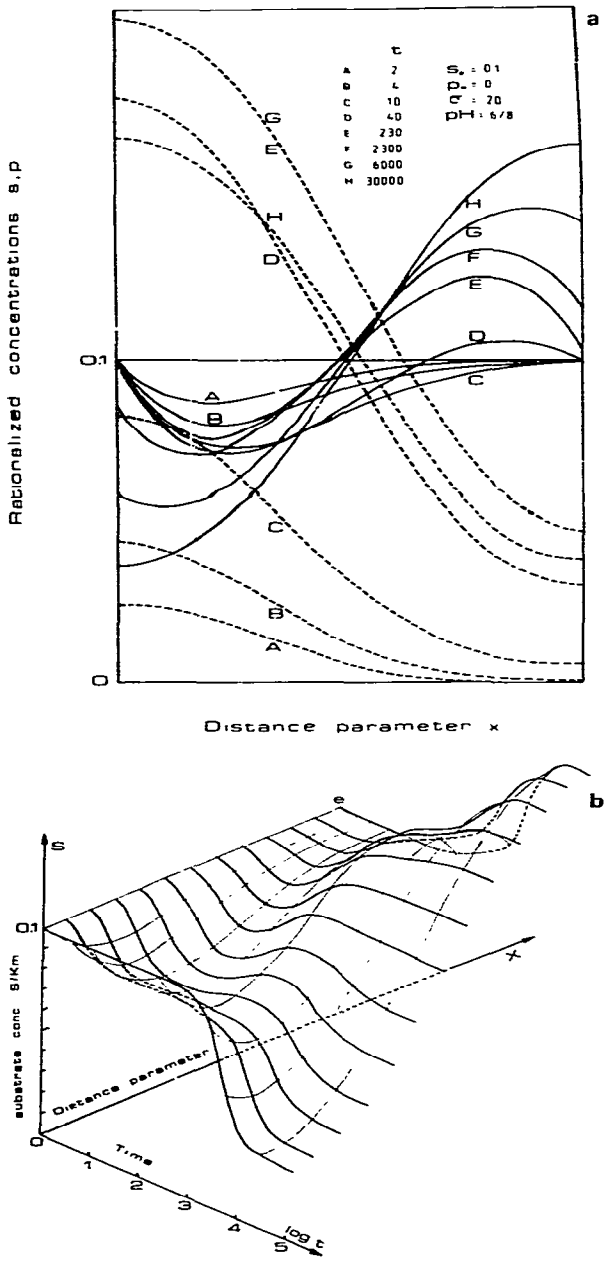

Fig. 11. Two-enzyme active transport membrane with a linear pH profile; initial conditions: membrane full of substrate and void of product (a) substrate (————) and product (— — —) concentration profiles at different real times; (b) three-dimensional substrate concentration evolutions as a function of distance parameter x and time (log t); numerical characteristics are the same as in (a).

global effective activities being the same for both enzymes, and the fluxes and gradients being controlled by this activity, the general properties of the "linear H^+" pump can also be represented by another equivalent square model with constant mean σ_1 and σ_2 activities in each layer.

The difference with the previous models is that in the present case the repartition of the activities as a function of x is asymmetrical as are the effective activity profiles, however, the global activities remain equal.

5. Some general remarks

Before the final discussion two important properties uniting all the models must be underlined in this section.

5.1. Time-dependent evolutions of $s(x, t)$ profiles

The $s(x, t)$ substrate concentration profile as a function of space and time coordinates covers a gauche twisted surface. An example of a membrane activated by a linear pH profile and initially full of substrate is given in fig. 11b.

With a sufficiently large cell/membrane volume ratio (v_c/v_m) during its establishment the pump first of all reaches the *working state* corresponding to unmodified boundaries. This working state is characterized by the *corresponding space wave* of the substrate concentration profile in the membrane. If, for example, the membrane is initially full of S, this oscillatory profile is formed by a progressive *deformation* of the initial profile (fig. 11). The profile remains unchanged as a function of time with infinite cell volumes (fixed boundaries) and the *state of the pump and the flux are steady.*

When v_c/v_m is finite this same established *state is quasi-stationary* and modifies itself according to the concentration modifications produced by the pump in the cells. The steady state is then defined

by a zero net flux through the membrane and depends on *the load* (ΔS) corresponding to the effective membrane activity in the *self-created* boundary conditions. The time required *to attain the steady state* depends on successive membrane activities and on cell volumes.

We note that the "unique" quasi-stationary state does not exist if v_c/v_m is so small that the simple filling of the membrane already changes the cell concentrations. Then the steady state will be attained following a shorter pathway dependent on the v_c/v_m factor (see fig. 5a).

All these conclusions are valid for all the models.

5.2. *The square and equivalent square models and the interdependence of effective enzyme activities*

The symmetrical square model proposed originally, in which equal $V(E_1)$ and $V(E_2)$ values were assumed, is a good approach when the active pH zones of E_1 and E_2 are very distinct and are respectively acid or alkaline.

The linear pH model is convenient when the active pH values approach 7 from different sides, but it is replaceable in the steady or quasi-stationary states by a symmetrical equivalent square model calculable from enzyme, membrane and boundary characteristics.

The linear H^+ model can also be reduced to an equivalent but asymmetrical model in the steady states even when the potential activities of the enzymes are different.

All this leads to the general conclusion that whatever the model, the nature of the pH gradient, the nature or ratios of potential enzyme activities, boundary conditions or profiles, the effective activities are equal in all steady states. They are virtually equal in the quasi-stationary states.

The conclusion is quite evident from the fact that the steady states are only possible if the consumption and production of S and P are equal and their profiles are maintained constant.

When the potential activities are unequal, a first-order activity of excess E_1 can be compensated by a zero-order action of a smaller amount of E_2. The inverse is also true but with some loss of pumping efficiency (table 2c).

Moreover, it appears to be verified that all evolutions tend toward equilibrated effective enzyme activities characterizing the steady state (see section 4.3.3.).

6. Discussion and conclusions

For more than ten years our group has been investigating in vitro active transports. We now wish to demonstrate that the interesting results expounded in this paper lead to more general conclusions which also include previous results.

The pump described belongs to the family of "primary molecule-motive" systems such as the "proton-motive" theory of Mitchell. It agrees with the Guggenheim-Mitchell principles [12,13] where a sink and a source reaction are linked by transport; it is completed with the theory of "inversible reactions" [1,4–6,9].

The greatest originality of this work was the insertion of enzymic properties into those of the pump. The enzymes bring the regulations through the pH and through the substrate and also as we previously demonstrated, the stereoselectivity [2,14]. In fact, in order to obtain isomer separation by the pump, we had to associate the molecular asymmetry (chirality) and the membrane asymmetry.

Where the membrane asymmetry is concerned, the "combined pH dependence" $\gamma_{1,2}$ (pH)—an intrinsic property of the enzyme mixture—brings the *pro-asymmetry* of the functional structure much as prochirality does toward chirality. The asymmetrical pH gradient (pH(x) function) imposed on the pro-asymmetrical mixture produces the functional structure ($V(E_{1,2})$ (x)) that may be called "latent asymmetry" of the membrane (in analogy with the photographical latent image). In the absence of substrate it is hard to identify this latent asymmetry which is "developed" by the combined effective activity ($V(\mathcal{E}_{1,2})$ when substrate is added and the asymmetrical substrate concentration space wave appears.

The singleness of steady state (for defined initial and boundary conditions) shows on the one hand the stability of these waves; on the other, it also demonstrates that these waves do not belong

to the family of non-linear "dissipative structures" that are predicted far from equilibrium [15]. On the contrary, with a low enzyme activity, space waves develop even without any substrate concentration difference between the boundaries, not far from equilibrium and well into the thermodynamic domain. With the trilogy of *"pro-asymmetry -latent asymmetry-developed asymmetry"* it can be considered that the enzyme structures "memorize" the properties that are necessary to obtain asymmetry and a high pump efficiency. The "asymmetrical space wave" (a whole number of waves) denomination was specifically introduced recently [1] (in agreement with the Brussels group) in order to underline the difference with "dissipative oscillatory profiles". Self-sustaining or self-destroying dissipative structures need feed-back regulations by products [9,16] which have been excluded here and which will be detailed later. However, we must insist on three points now.

First, let us consider pH gradients. In the present model the pH gradient of *sine qua non* necessity is the inductor of asymmetry. But even if the two enzymes were distributed in two separate layers, as in the "permanent structure" model already studied [3,17] and not intimately mixed, a pH difference between these layers would nevertheless be necessary for the pump to work if the $\gamma_1(pH)$ and $\gamma_2(pH)$ functions do not overlap each other. The necessity of such a ΔpH due to enzyme properties is often overlooked by those who discuss the problem in biological terms. We can conclude that calculation of potential enzyme activities is a complement which is also beneficial for "permanent structures".

Secondly, the steady-state equality $V(\mathfrak{S}_1) = V(\mathfrak{S}_2)$—or in other words the definition of this state by zero "combined effective activity" ($V(\mathfrak{S}_{1,2}) = 0$) — and the resulting "equivalent square models" can describe the pump in very general terms that are perfectly consistent with the methods of irreversible thermodynamics, independent of the "functional", "permanent" or "mixed" nature of the enzyme activity structure. Such descriptions are valid even when the space wave is strongly deformed by lack of isotropy or convective contributions [4].

Thirdly, the molecule-motive-two-reaction model is valid for charged as well as uncharged species; in Mitchell's terms "charge would be incidental" [12]. Molecules, ions or electrons can be moved between "sink" and "source"; for example, an H^+ pumping model has recently been studied [9]. Moreover, with the "reaction products" hot and cold respectively, *enzymic* (Michaelian) *heat pumps* can be designed. Such pumps can use the sink and the source reactions. We feel we are justified in using the term "generalized sinks and sources" and qualify this primary active transport of *"chemical equivalent of heat pumps"*. The mathematical description would not undergo major modifications as long as the "primary" chemical potential (affinity) forces are not significantly perturbed by additional (electrical potential, pressure) forces.

The very reasonable agreement between calculated and experimental effects and results, the availability of heat pump mathematics and the demonstration of non-enzymatic pumps [4] lead us to the conclusion that "coupled primary pumps" transporting several types of species must bring more information [9,16] before deeper exploration of the more recent "time oscillation" active transport [6,9] and of primary-secondary coupling.

Last but not least, we are particularly happy that this research has already brought about [18,19] new progress in computer-connected fermentations used to detect and study bacterial growth and activity.

References

[1] E. Selegny and J.C. Vincent, Biophys. Chem. 12 (1980) 93.
[2] E. Selegny and J.C. Vincent, Biophys. Chem. 12 (1980) 107.
[3] E. Selegny, in: Polyelectrolytes, eds. E. Selegny, M. Mandel and U.P. Strauss (Reidel, Dordrecht, 1974) p419.
[4] E. Selegny and D. Langevin, J. Chem. Res. (1978) 278 (S) 3466 (M).
[5] E. Selegny and J.C. Vincent, J. Chim. Phys. 77 (1980) 1083.
[6] J.C. Vincent and E. Selegny, Compt. Rend. Acad. Sci. Paris Ser. III, 292 (1981) 173.
[7] E. Selegny, J.P. Kernevez, G. Broun and D. Thomas, Physiol. Veg. 9 (1971) 25.
[8] J.P. Kernevez, Thesis Dr. Sci., Paris 1972; in: Enzyme mathematics, eds. J.L. Lions, G. Papanicolau and R.T. Rockafellar (North-Holland, Amsterdam, 1980).

[9] J.C. Vincent, Thesis Dr. Sci., Rouen 1980.
[10] J.M. Valleton, J.C. Vincent and E. Selegny, Biophys. Bioeng. submitted.
[11] D. Langevin, M. Metayer, J. Mousnitskas and E. Selegny, J. Chim. Phys., to be published.
[12] P. Mitchell, Chemiosmotic coupling and energy transduction (Glynn Res. Ltd. Bodmin, 1968).
[13] E.A. Guggenheim, Modern thermodynamics by the methods of Willard–Gibbs (Methuen, London, 1933).
[14] E. Selegny, J.C. Vincent and M. Lancon, Tetrahedron lett. 33 (1977) 3171.
[15] P. Glansdorff and I. Prigogine, Structure, stabilité et fluctuations (Masson, Paris, 1971).
[16] J.C. Vincent and E. Selegny, J. Non-Equilibrium Thermodyn., submitted.
[17] E. Selegny, G. Broun and D. Thomas, Compt. Rend. Acad. Sci. Paris 271 D (1970) 1423.
[18] G.A. Junter, J.F. Lemeland and E. Selegny, Appl. Environm. Microbiol., 39(2) (1980) 307.
[19] G.A. Junter, E. Selegny and J.F. Lemeland, Ann. Microbiol. (Inst. Pasteur) 130A (1979) 295.